

K^* resonance effects on direct CP violation in $B \rightarrow \pi\pi K$ O. Leitner,¹ J.-P. Dedonder,¹ B. Loiseau,¹ and R. Kamiński²¹*Laboratoire de Physique Nucléaire et de Hautes Énergies (IN2P3–CNRS–Universités Paris 6 et 7), Groupe Théorie, Universités Pierre et Marie Curie et Paris-Diderot, 4 place Jussieu, 75252 Paris, France*²*Division of Theoretical Physics, The Henryk Niewodniczański Institute of Nuclear Physics, Polish Academy of Sciences, 31-342 Kraków, Poland*

(Received 28 January 2010; published 27 May 2010)

$B^\pm \rightarrow \pi^+ \pi^- K^\pm$ and $\bar{B}^0 \rightarrow \pi^+ \pi^- \bar{K}^0$ decay channels are analyzed within the QCD factorization scheme where final state interactions before and after hadronization are included. The $K^*(892)$ and $K_0^*(1430)$ resonance effects are taken into account using the presently known πK strange vector and scalar form factors. The weak decay amplitudes, which are calculated at leading power in Λ_{QCD}/m_b and at the next-to-leading order in the strong coupling constant, include the hard-scattering and annihilation contributions. The end-point divergences of these weak final state interactions are controlled by two complex parameters determined through a fit to the available effective mass and helicity angle distribution, CP asymmetry, and $K^*(892)$ branching ratio data. The predicted $K_0^*(1430)$ branching ratios and the calculated direct CP violation asymmetries are compared to the Belle and BABAR Collaboration data.

DOI: 10.1103/PhysRevD.81.094033

PACS numbers: 13.25.Hw, 11.30.Er

I. INTRODUCTION

In the standard model, it is known that CP violation is mainly predicted in weak decays because of the weak phase of the Cabibbo-Kobayashi-Maskawa (CKM) matrix [1]. In decays of B mesons, through electroweak interaction, one can calculate the matter–antimatter asymmetry; W -boson exchange and large beauty quark mass allow a systematic perturbative calculation in the QCD factorization formalism (QCDF) [2] where the final state interactions are the main source of uncertainty. It is the combined occurrence of a weak and a strong phase difference that leads to the observation of the CP violating asymmetry between the $B \rightarrow \pi^\pm \pi^\mp K$ and $\bar{B} \rightarrow \pi^\mp \pi^\pm \bar{K}$ channels.

Electroweak decays of resonant and nonresonant mesons made of a $q\bar{q}$ pair are well described in QCDF. In this framework, there is no direct three-body factorization scheme that efficiently describes a three-body decay, hence a quasi-two-body state has first to be built up. Here, one of the two mesons assumed to be a K^* resonance can decay via a strong decay mechanism to a (πK) state. In Ref. [3], the authors attempt to reproduce the πK effective mass and helicity angle distributions. In that calculation, the weak amplitude relies on effective QCD coefficients describing the leading order (LO) contribution as well as the vertex and penguin corrections at the order of Λ_{QCD}/m_b . The K^* resonances decaying into πK are then modeled by the scalar and vector form factors [4] that correspond to the strong final state interactions after hadronization. Additional phenomenological amplitudes, represented by four complex free parameters and added to the QCD penguin amplitude, are fitted to mainly reproduce the $B \rightarrow K^*(892)\pi$ branching ratio and the CP asymmetry of the recent Belle and BABAR Collaboration data. Furthermore they also predict the $B \rightarrow K^*(1430)\pi$ branching ratio.

Altogether, one obtains a fair description of the data for these three-body B decays.

In the present work, one explicitly includes the hard-scattering and annihilation corrections at the order of Λ_{QCD}/m_b . These weak final state interactions based on phenomenological assumptions are controlled by the end-point divergences related to the asymptotic wave functions. This approach reduces thus the number of free parameters to only two complex ones.

In Sec. II, we derive the three-body decay amplitudes for the $B \rightarrow \pi\pi K$ processes within the QCDF framework introducing quasi-two-body states. Sections III and IV provide all the details for the weak decay amplitudes calculated at next-to-leading order in the strong coupling constant and in the perturbative expansion of the short distance interaction for $B \rightarrow \pi K^*(892)$ and $B \rightarrow \pi K_0^*(1430)$. Section V lists all the numerical parameters employed and in Sec. VI a discussion follows the presentation of the significant results on branching ratios and asymmetries. Finally, Sec. VII concludes with a summary of our work and some outlook.

II. THREE-BODY DECAY AMPLITUDE

To analyze the $B \rightarrow \pi\pi K$ decay amplitude, one first evaluates the matrix element $\langle \pi M_2 | \mathcal{H}_{\text{eff}} | B \rangle$ within the factorization hypothesis,

$$\begin{aligned} \langle \pi M_2 | \mathcal{H}_{\text{eff}} | B \rangle &\propto \langle M_2 | \bar{s} \gamma_\nu (1 - \gamma_5) d | 0 \rangle \\ &\times \langle \pi | \bar{u} \gamma^\nu (1 - \gamma_5) b | B \rangle, \end{aligned} \quad (1)$$

with M_2 being either the vector $K^*(892)$ or scalar $K_0^*(1430)$ resonance, and \mathcal{H}_{eff} is the standard effective Hamiltonian for B decay (see Ref. [3]). The vector $K^*(892)$ and the scalar $K_0^*(1430)$ resonances are assumed to be (πK) quasi-bound states in P and S waves, respectively. Thus, one

writes [3]

$$\langle \pi \pi K | \mathcal{H}_{\text{eff}} | B \rangle \propto \langle (\pi K)_{S,P} | \bar{s} \gamma_\nu (1 - \gamma_5) d | 0 \rangle \times \langle \pi | \bar{u} \gamma^\nu (1 - \gamma_5) b | B \rangle, \quad (2)$$

where $\langle (\pi K)_{S,P} | \bar{s} \gamma_\nu (1 - \gamma_5) d | 0 \rangle$ is expressed as

$$\begin{aligned} & \langle \pi(p_\pi) K(p_K) | \bar{s} \gamma_\nu (1 - \gamma_5) d | 0 \rangle \\ &= \left[(p_K - p_\pi)_\nu - \frac{m_K^2 - m_\pi^2}{q^2} q_\nu \right] f_1^{\pi K}(q^2) \\ &+ \frac{m_K^2 - m_\pi^2}{q^2} q_\nu f_0^{\pi K}(q^2). \end{aligned} \quad (3)$$

In Eq. (3), q^2 with $q = p_K + p_\pi$ is the invariant πK mass squared, and m_K and m_π denote the kaon and pion masses, respectively. The vector $f_1^{\pi K}(q^2)$ and scalar $f_0^{\pi K}(q^2)$ form factors are describing the final state interaction after hadronization. From semileptonic decays like $\tau \rightarrow K \pi \nu_\tau$ and $K \rightarrow \pi l \nu_l$, one can extract information on these $K \pi$ scalar and vector form factors [4]. Analyticity, unitarity, QCD counting asymptotic rules allow one to relate scalar and vector form factors to the $K_0^*(1430) \rightarrow \pi K$ and $K^*(892) \rightarrow \pi K$ scattering amplitudes in the elastic and inelastic domains. All the details can be found in Refs. [3,4]. The full amplitude for each wave is given by

$$\mathcal{A}_3(B \rightarrow \pi \pi K) = \mathcal{A}(B \rightarrow \pi M_2) \times \Gamma(M_2 \rightarrow K \pi). \quad (4)$$

For the $K^*(892)$, the vertex function $\Gamma(K^*(892) \rightarrow K \pi)$

associated with the $B \rightarrow \pi K^* \rightarrow \pi \pi K$ decay is written as

$$\Gamma(K^*(892) \rightarrow K \pi) = \frac{2}{q f_{K^*}} \frac{\mathbf{p}_{\pi^+} \cdot \mathbf{p}_{\pi^-}}{\epsilon_{K^*(892)}^* \cdot p_B} f_1^{\pi K}(q^2), \quad (5)$$

where f_{K^*} is the K^* decay constant and $\epsilon_{K^*(892)}^* \cdot p_B = (m_B/2q) \lambda^{1/4}(m_B^2, q^2, m_\pi^2)$, p_B and m_B denoting the B four momentum and mass, respectively. In Eq. (5), $\lambda(x, y, z) = (x + y - z)^2 - 4xy$ and the moduli of the π^\pm momenta are

$$|\mathbf{p}_{\pi^+}| = \frac{1}{2q} \sqrt{[q^2 - (m_K + m_\pi)^2][q^2 - (m_K - m_\pi)^2]}, \quad (6)$$

and

$$|\mathbf{p}_{\pi^-}| = \frac{1}{2q} \sqrt{[m_B^2 - (q + m_\pi)^2][m_B^2 - (q - m_\pi)^2]}. \quad (7)$$

The vertex function $\Gamma(K_0^*(1430) \rightarrow K \pi)$ is

$$\Gamma(K_0^*(1430) \rightarrow K \pi) = \frac{1}{f_{K_0^*}} \frac{m_K^2 - m_\pi^2}{q^2} f_0^{\pi K}(q^2), \quad (8)$$

where $f_{K_0^*}$ denotes the K_0^* decay constant. Following closely [2], one derives the QCDF decay amplitudes where the short and long distance contributions are factorized in the approximation of a quasi-two-body state, $\pi K^*(892)$ or $\pi K_0^*(1430)$.

The amplitude $B^- \rightarrow \pi^- \bar{K}^{*0}(892)$ is

$$\begin{aligned} \mathcal{A}(B^- \rightarrow \pi^- \bar{K}^{*0}) &= \sum_{q=u,c} \lambda_q^{(s)} \left\{ A_{\pi K^*} \left[\delta_{qu} \beta_2(\mu) + a_4^q(\mu) + r_\chi^{K^*}(\mu) a_6^q(\mu) \right. \right. \\ &\quad \left. \left. - \frac{1}{2} (a_{10}^q(\mu) + r_\chi^{K^*}(\mu) a_8^q(\mu)) + \beta_3(\mu) + \beta_{3,\text{EW}}(\mu) \right]_{\pi K^*} \right\}, \end{aligned} \quad (9)$$

and the $\bar{B}^0 \rightarrow \pi^+ \bar{K}^{*-}(892)$ amplitude,

$$\begin{aligned} \mathcal{A}(\bar{B}^0 \rightarrow \pi^+ \bar{K}^{*-}) &= \sum_{q=u,c} \lambda_q^{(s)} \left\{ A_{\pi K^*} \left[\delta_{qu} a_1^q(\mu) + a_4^q(\mu) + r_\chi^{K^*}(\mu) a_6^q(\mu) + a_{10}^q(\mu) + r_\chi^{K^*}(\mu) a_8^q(\mu) + \beta_3(\mu) \right. \right. \\ &\quad \left. \left. - \frac{1}{2} \beta_{3,\text{EW}}(\mu) \right]_{\pi K^*} \right\}, \end{aligned} \quad (10)$$

where the coefficients $a_n^q(\mu)$ and $\beta_n(\mu)$ are given in Eqs. (18) and (20). The $\lambda_q^{(s)}$ are a product of CKM matrix elements, the $r_\chi^{M_2}(\mu)$ the chiral coefficients, and μ is the scale.

The $B^- \rightarrow \pi^- \bar{K}_0^{*0}(1430)$ amplitude reads

$$\begin{aligned} \mathcal{A}(B^- \rightarrow \pi^- \bar{K}_0^{*0}) &= \sum_{q=u,c} \lambda_q^{(s)} \left\{ A_{\pi K_0^*} \left[\delta_{qu} \beta_2(\mu) + a_4^q(\mu) - r_\chi^{K_0^*}(\mu) a_6^q(\mu) \right. \right. \\ &\quad \left. \left. - \frac{1}{2} (a_{10}^q(\mu) - r_\chi^{K_0^*}(\mu) a_8^q(\mu)) + \beta_3(\mu) + \beta_{3,\text{EW}}(\mu) \right]_{\pi K_0^*} \right\}, \end{aligned} \quad (11)$$

while the $\bar{B}^0 \rightarrow \pi^+ K_0^{*-}(1430)$ amplitude is

$$\mathcal{A}(\bar{B}^0 \rightarrow \pi^+ K_0^{*-}) = \sum_{q=u,c} \lambda_q^{(s)} \left\{ A_{\pi K_0^*} \left[\delta_{qu} a_1^q(\mu) + a_4^q(\mu) - r_{\chi}^{K_0^*}(\mu) a_6^q(\mu) + a_{10}^q(\mu) - r_{\chi}^{K_0^*}(\mu) a_8^q(\mu) + \beta_3(\mu) - \frac{1}{2} \beta_{3,EW}(\mu) \right]_{\pi K_0^*} \right\}. \quad (12)$$

The chiral coefficients, $r_{\chi}^{K^*}(\mu)$ and $r_{\chi}^{K_0^*}(\mu)$, will be given in Eqs. (24) and (40).

For the $K^*(892)$ resonance, the pseudoscalar-vector factor $A_{\pi K^*}$ in Eqs. (9) and (10) reads

$$A_{\pi K^*} = -i \frac{G_F}{\sqrt{2}} 2q \epsilon_{K^*(892)}^* \cdot p_B F_0^{B \rightarrow \pi}(q^2) f_{K^*}, \quad (13)$$

with the Fermi constant $G_F = 1.16 \times 10^{-5} \text{ GeV}^{-2}$ and where the weak transition form factor $F_0^{B \rightarrow \pi}(q^2)$ will be given in Sec. V. For the $K_0^*(1430)$ scalar resonance, the pseudoscalar-scalar factor $A_{\pi K_0^*}$ in Eqs. (11) and (12) is

$$A_{\pi K_0^*} = i \frac{G_F}{\sqrt{2}} (m_B^2 - m_{\pi}^2) F_0^{B \rightarrow \pi}(q^2) f_{K_0^*}. \quad (14)$$

In Eqs. (9)–(12), the CKM matrix elements are

$$\begin{aligned} \lambda_u^{(s)} &= V_{ub} V_{us}^* = A \lambda^3 (\rho - i \eta) \lambda, \\ \lambda_c^{(s)} &= V_{cb} V_{cs}^* = A \lambda^2 \left(1 - \frac{\lambda^2}{2} \right), \end{aligned} \quad (15)$$

where following Ref. [5] the Wolfenstein parameters are $A = 0.814$, $\rho = 0.1385$, $\eta = 0.358$, and $\lambda = 0.2257$.

Since one assumes the dominance of the $K^*(892)$ and $K_0^*(1430)$ resonances in the description of the πK channel, the full amplitude $\mathcal{A}_3(B \rightarrow \pi \pi K)$ is built up on the P and S waves so that the differential effective mass branching fraction is [3]

$$\frac{d\mathcal{B}(B \rightarrow \pi \pi K)}{dq} = \frac{1}{\Gamma_B} \frac{q |\mathbf{p}_{\pi^+}||\mathbf{p}_{\pi^-}|}{4(2\pi)^3 m_B^3} \left(|\mathcal{A}_3(B \rightarrow \pi(\pi K)_S)|^2 + \frac{1}{3} |\mathcal{A}_3(B \rightarrow \pi(\pi K)_P)|^2 \right), \quad (16)$$

where $\Gamma_B = 1/\tau_B$ is the B -decay width. The usual CP violating asymmetry parameter is

$$\mathbb{A}_{CP}(B \rightarrow \pi \pi K) = \frac{\mathcal{B}(B \rightarrow \pi \pi K) - \mathcal{B}(\bar{B} \rightarrow \bar{\pi} \bar{\pi} \bar{K})}{\mathcal{B}(B \rightarrow \pi \pi K) + \mathcal{B}(\bar{B} \rightarrow \bar{\pi} \bar{\pi} \bar{K})}. \quad (17)$$

In Eqs. (9)–(12), the $a_n^q(\mu)$, involving the Wilson coefficients $C_n(\mu)$, are

$$\begin{aligned} a_n^q(\mu) &= \left[C_n(\mu) + \frac{C_{n\pm 1}(\mu)}{N_c} \right] N_n(M_2) + P_n^q(M_2) \\ &+ \frac{C_f}{4\pi N_c} \left[\alpha_s(\mu) C_{n\pm 1}(\mu) V_n(M_2) \right. \\ &\left. + \frac{4\pi^2 \alpha_s(\mu/2)}{N_c} C_{n\pm 1}(\mu/2) H_n(\pi M_2) \right], \end{aligned} \quad (18)$$

with $n \in \{1, 10\}$, and the scale is $\mu = m_b$, with m_b being the b quark mass. In Eq. (18), the color number is $N_c = 3$ and $C_f = (N_c^2 - 1)/2N_c = 4/3$. The upper (lower) signs in $C_{n\pm 1}(\mu)$ apply when n is odd (even) and

$$N_n(M_2) = \begin{cases} 0, & n \in \{6, 8\}, \text{ and } M_2 \equiv K^*(892), \\ 1, & \text{else.} \end{cases} \quad (19)$$

The Wilson coefficients, $C_n(\mu)$, computed in the naive dimension regularization (NDR) scheme [2], are taken at the scale m_b for the vertex, $V_n(M_2)$, and penguin $P_n^q(M_2)$, corrections which involve only the b quark, whereas the annihilation, $\beta_n(\pi M_2)$ and hard scattering, $H_n(M_2)$, contributions are evaluated at the scale $m_b/2$ since they involve the spectator quark. The strong coupling constants are $\alpha_s(m_b) = 0.224$ and $\alpha_s(m_b/2) = 0.286$ [5].

The annihilation term, $\beta_n(\mu)$, is given by

$$[\beta_n(\mu)]_{\pi M_2} = \frac{[b_n(\mu)]_{\pi M_2} B_{\pi M_2}}{A_{\pi M_2}}, \quad (20)$$

where the factor, $B_{\pi M_2}$, is the product of G_F by the B , π , and M_2 decay constants,

$$B_{\pi M_2} = \mp i \frac{G_F}{\sqrt{2}} f_B f_{\pi} f_{M_2}, \quad (21)$$

with the upper sign if $M_2 \equiv K^*(892)$ and the lower sign otherwise. In Eqs. (9)–(12), the tree annihilation component (at $\mu = m_b/2$) is (the upper scripts I and F denote initial and final states)

$$[b_2(\mu)]_{\pi M_2} = \frac{C_f}{N_c^2} C_2(\mu) A_1^I(\pi M_2), \quad (22)$$

while the penguin annihilation terms (at $\mu = m_b/2$) are

$$\begin{aligned} [b_3(\mu)]_{\pi M_2} &= \frac{C_f}{N_c^2} [C_3(\mu) A_1^I(\pi M_2) \\ &+ C_5(\mu) (A_3^I(\pi M_2) + A_3^F(\pi M_2)) \\ &+ N_c C_6(\mu) A_3^F(\pi M_2)], \\ [b_{3,EW}(\mu)]_{\pi M_2} &= \frac{C_f}{N_c^2} [C_9(\mu) A_1^I(\pi M_2) \\ &+ C_7(\mu) (A_3^I(\pi M_2) + A_3^F(\pi M_2)) \\ &+ N_c C_8(\mu) A_3^F(\pi M_2)], \end{aligned} \quad (23)$$

where the amplitudes $A_j^{I,F}(\pi M_2)$ are given in Eqs. (36) for the P wave and (50) for the S wave.

III. QCDF CORRECTIONS FOR $B \rightarrow \pi K^*$ (892)

The pion in the final state πK^* (892) is created from the transition $B \rightarrow \pi$ while the K^* (892) is created from the vacuum; this mechanism is due to the structure of the four-quark operators in the heavy quark effective theory as well as the conservation of the flavor quantum numbers. Following Ref. [2], we only give the QCD corrections that appear in $\mathcal{A}(B \rightarrow \pi K^*$ (892)).

Since the coefficients in the Gegenbauer expansion of the light cone distribution amplitudes (LCDA) are known with large uncertainties [2], one here limits oneself to leading terms in this expansion for the π and K^* (892). The leading twist-2 distribution amplitude is $\Phi(x) = 6x(1-x)$ and the twist-3 two particle distribution is $\varphi(x) = 1$ and $\varphi(x) = 3(2x-1)$ for both π and K^* (892).

The chiral coefficient for the vector meson K^* (892), given at the scale μ , is defined as

$$r_{\chi}^{K^*}(\mu) = \frac{2\sqrt{q^2} f_{K^*}^\perp}{m_b(\mu) f_{K^*}}, \quad (24)$$

where $f_{K^*}^\perp$ is the transverse decay constant and where one has introduced the running meson mass square, replacing $m_{K^*(892)}^2$ by $m_{\pi K}^2 = q^2$. For a pion, the chiral coefficient reads

$$r_{\chi}^{\pi}(\mu) = \frac{m_{\pi}^2}{m_b(\mu)m_u(\mu)}, \quad (25)$$

with the u -quark mass m_u .

A. Penguin contributions

The penguin contributions, $P_n^q(K^*(892))$, with the values $n = 4, 6, 8, 10$, required in Eqs. (9) and (10), are as follows:

$$\begin{aligned} P_4^q(K^*(892)) &= \frac{C_f \alpha_s(\mu)}{4\pi N_c} \left\{ C_1(\mu) \left[\frac{4}{3} \ln \frac{m_b}{\mu} + \frac{2}{3} - G_{K^*(892)}(s_q) \right] + C_3(\mu) \left[\frac{8}{3} \ln \frac{m_b}{\mu} + \frac{4}{3} - G_{K^*(892)}(0) - G_{K^*(892)}(1) \right] \right. \\ &\quad + (C_4(\mu) + C_6(\mu)) \left[\frac{4n_F}{3} \ln \frac{m_b}{\mu} - (n_F - 2)G_{K^*(892)}(0) - G_{K^*(892)}(s_c) - G_{K^*(892)}(1) \right] \\ &\quad \left. - 2C_{8g}^{\text{eff}}(\mu) \int_0^1 \frac{dx}{1-x} \Phi_{K^*(892)}(x) \right\}, \end{aligned} \quad (26)$$

with

$$\int_0^1 \frac{dx}{1-x} \Phi_{K^*(892)}(x) = 3, \quad (27)$$

and $C_{8g}^{\text{eff}}(\mu)$ related to the Q_{8g} chromomagnetic dipole operator. Furthermore,

$$\begin{aligned} P_6^q(K^*(892)) &= \frac{C_f \alpha_s(\mu)}{4\pi N_c} \left\{ C_1(\mu) \hat{G}_{K^*(892)}(s_q) + C_3(\mu) [\hat{G}_{K^*(892)}(0) - \hat{G}_{K^*(892)}(1)] \right. \\ &\quad \left. + (C_4(\mu) + C_6(\mu)) [(n_F - 2)\hat{G}_{K^*(892)}(0) - \hat{G}_{K^*(892)}(s_c) - \hat{G}_{K^*(892)}(1)] \right\}, \end{aligned} \quad (28)$$

$$P_8^q(K^*(892)) = -\frac{\alpha_e}{9\pi N_c} (C_1(\mu) + N_c C_2(\mu)) \hat{G}_{K^*(892)}(s_q), \quad (29)$$

where $\alpha_e = 1/129$ is the electromagnetic coupling constant. Finally,

$$P_{10}^q(K^*(892)) = \frac{\alpha_e}{9\pi N_c} \left\{ (C_1(\mu) + N_c C_2(\mu)) \left[\frac{4}{3} \ln \frac{m_b}{\mu} + \frac{2}{3} - G_{K^*(892)}(s_q) \right] - 3C_{7\gamma}^{\text{eff}}(\mu) \int_0^1 \frac{dx}{1-x} \Phi_{K^*(892)}(x) \right\}. \quad (30)$$

In these equations, $\mu = m_b$ and the number of active flavors is $n_F = 5$. In Eq. (30), $C_{7\gamma}^{\text{eff}}(\mu)$ is related to the $Q_{7\gamma}$ electromagnetic dipole operator. The gluon kernel contributions are

$$G_{K^*(892)}(s_q) = \begin{cases} \frac{5}{3} + \frac{2i\pi}{3}, & s_q = 0, \\ \frac{85}{3} - 6\sqrt{3}\pi + \frac{4\pi^2}{9}, & s_q = 1, \\ \frac{5}{3} - \frac{2}{3} \ln s_c + \frac{32}{3} s_c + 16s_c^2 - \frac{2}{3} \sqrt{1-4s_c} [1 + 2s_c + 24s_c^2] [2 \operatorname{arctanh}(\sqrt{1-4s_c}) \\ - i\pi] + 12s_c^2 (1 - \frac{4}{3} s_c) [2 \operatorname{arctanh}(\sqrt{1-4s_c}) - i\pi]^2, & s_q = s_c, \end{cases} \quad (31)$$

and

$$\hat{G}_{K^*(892)}(s_q) = \begin{cases} 1, & s_q = 0, \\ -35 + 4\sqrt{3}\pi + \frac{4\pi^2}{3}, & s_q = 1, \\ -12s_c^2[2 \operatorname{arctanh}(\sqrt{1-4s_c}) - i\pi]^2 - 36s_c \\ + 12\sqrt{1-4s_c}s_c[2 \operatorname{arctanh}(\sqrt{1-4s_c}) - i\pi] + 1, & s_q = s_c. \end{cases} \quad (32)$$

In Eqs. (31) and (32), s_q is defined as $(m_q/m_b)^2$ so that $s_q = 0$ for $q = u, d$, $s_q = 1$ for $q = b$, and $s_q = s_c$ for $q = c$.

B. Vertex contributions

In the $B \rightarrow \pi K^*(892)$ transition, the electroweak vertex, $V_n(K^*(892))$, receives $\alpha_s(\mu)$ corrections to all $a_n^q(\mu)$ in the amplitude $\mathcal{A}(B \rightarrow \pi K^*(892))$,

$$V_n(K^*(892)) = \begin{cases} 12 \ln(\frac{m_b}{\mu}) - 3i\pi - \frac{37}{2}, & n \in \{1, 4, 10\}, \\ 9 - 6i\pi, & n \in \{6, 8\}. \end{cases} \quad (33)$$

C. Hard-scattering contributions

Evaluated at the scale $\mu = m_b/2$, the hard-scattering correction can be written as

$$H_n(\pi M_2) = \frac{B_{\pi M_2}}{A_{\pi M_2}} \tilde{H}_n(\pi M_2), \quad (34)$$

where for the vector resonance, $M_2 \equiv K^*(892)$, $A_{\pi K^*(892)}$,

$$\begin{aligned} A_1^I(\pi K^*(892)) &\approx 6\pi\alpha_s(\mu) \left[3 \left(X_A - 4 + \frac{\pi^2}{3} \right) + r_\chi^{K^*}(\mu) r_\chi^\pi(\mu) (X_A^2 - 2X_A) \right], \\ A_3^I(\pi K^*(892)) &\approx 6\pi\alpha_s(\mu) \left[-3r_\chi^{K^*}(\mu) \left(X_A^2 - 2X_A - \frac{\pi^2}{3} + 4 \right) + r_\chi^\pi(\mu) \left(X_A^2 - 2X_A + \frac{\pi^2}{3} \right) \right], \\ A_3^F(\pi K^*(892)) &\approx -6\pi\alpha_s(\mu) [3r_\chi^{K^*}(\mu)(2X_A - 1)(2 - X_A) - r_\chi^\pi(\mu)(2X_A^2 - X_A)], \end{aligned} \quad (36)$$

with $\mu = m_b/2$.

IV. QCDF CORRECTIONS FOR $B \rightarrow \pi K_0^*(1430)$

We now turn to the $B \rightarrow \pi K_0^*(1430)$ transition for which the $\alpha_s(\mu)$ corrections are all included. Here again, only the first nonvanishing leading term in the LCDA of the $K_0^*(1430)$ are retained:

$$\Phi_{K_0^*(1430)}(x) = 6x(1-x)[1 + 3B_1^{K_0^*(1430)}(\mu)(2x-1)], \quad (37)$$

where $B_1^{K_0^*(1430)}(\mu = m_b) = 5.26$, and $B_1^{K_0^*(1430)}(\mu = m_b/2) = 0.39$ are the first nonvanishing Gegenbauer moments (for neutral scalar) evaluated at two different mass scales. The asymptotic form of the LCDA for the pion is

$$\Phi_\pi(x) = 6x(1-x). \quad (38)$$

and $B_{\pi K^*(892)}$ are defined by Eqs. (13) and (21), respectively. One has

$$\tilde{H}_n(\pi K^*(892)) = \begin{cases} 3 \frac{m_B}{\lambda_B} [r_\chi^\pi(\mu) X_H + 3], & n \in \{1, 4, 10\}, \\ 0, & n \in \{6, 8\}, \end{cases} \quad (35)$$

where $\lambda_B = 0.3$ GeV is a hadronic parameter of the order of Λ_{QCD} [6]. In Eq. (35), $r_\chi^\pi(\mu)$ is given by Eq. (25) and X_H represents the end-point divergence related to the soft-gluon interaction with the spectator quark. Its expression will be given in Eq. (56) in Sec. V.

D. Annihilation contributions

The annihilation amplitudes cannot be derived from the QCDF approach so that they are model dependent involving also a divergence parametrized by X_A [Eq. (56)]. Based on Ref. [2], the expressions for $A_j^I(\pi K^*(892))$ and $A_j^F(\pi K^*(892))$, for $j = 1$ and 3, are

The twist-3 two particle distributions are

$$\varphi_{K_0^*(1430)}(x) = 1 \quad \text{and} \quad \varphi_\pi(x) = 1. \quad (39)$$

Similarly to the $B \rightarrow \pi K^*(892)$ decay channel, the $B \rightarrow \pi K_0^*(1430)$ decay amplitude is factorized out into a product of a transition form factor $B \rightarrow \pi$ times a $K_0^*(1430)$ decay constant as shown in Eq. (2) of Ref. [2].

The $K_0^*(1430)$ chiral coefficient is given by

$$r_\chi^{K_0^*(1430)}(\mu) = \frac{2q^2}{m_b(\mu)(m_s(\mu) - m_u(\mu))}, \quad (40)$$

where m_s is the strange quark mass. In Eq. (40), as has been done for the $K^*(892)$ meson [see Eq. (24)], one has introduced the running meson mass square for the $K_0^*(1430)$ replacing $m_{K_0^*(1430)}^2$ by $m_{\pi K}^2 = q^2$.

A. Penguin contributions

From Ref. [2], one can obtain all the penguin corrections $P_n^q(K_0^*(1430))$ (with $n = 4, 6, 8, 10$) for the B to pseudoscalar-scalar transition. One has

$$P_4^q(K_0^*(1430)) = \frac{C_f \alpha_s(\mu)}{4\pi N_c} \left\{ C_1(\mu) \left[\frac{4}{3} \ln \frac{m_b}{\mu} + \frac{2}{3} - G_{K_0^*(1430)}(s_q) \right] + C_3(\mu) \left[\frac{8}{3} \ln \frac{m_b}{\mu} + \frac{4}{3} - G_{K_0^*(1430)}(0) - G_{K_0^*(1430)}(1) \right] \right. \\ \left. + (C_4(\mu) + C_6(\mu)) \left[\frac{4n_F}{3} \ln \frac{m_b}{\mu} - (n_F - 2)G_{K_0^*(1430)}(0) - G_{K_0^*(1430)}(s_c) - G_{K_0^*(1430)}(1) \right] \right. \\ \left. - 2C_{8g}^{\text{eff}}(\mu) \int_0^1 \frac{dx}{1-x} \Phi_{K_0^*(1430)}(x) \right\}, \quad (41)$$

with

$$\int_0^1 \frac{dx}{1-x} \Phi_{K_0^*(1430)}(x) = 3B_1^{K_0^*}(\mu) + 3. \quad (42)$$

Moreover,

$$P_6^q(K_0^*(1430)) = \frac{C_f \alpha_s(\mu)}{4\pi N_c} \left\{ C_1(\mu) \left[\frac{4}{3} \ln \frac{m_b}{\mu} + \frac{2}{3} - \hat{G}_{K_0^*(1430)}(s_q) \right] + C_3(\mu) \left[\frac{8}{3} \ln \frac{m_b}{\mu} + \frac{4}{3} - \hat{G}_{K_0^*(1430)}(0) - \hat{G}_{K_0^*(1430)}(1) \right] \right. \\ \left. + (C_4(\mu) + C_6(\mu)) \left[\frac{4n_F}{3} \ln \frac{m_b}{\mu} - (n_F - 2)\hat{G}_{K_0^*(1430)}(0) - \hat{G}_{K_0^*(1430)}(s_c) - \hat{G}_{K_0^*(1430)}(1) \right] - 2C_{8g}^{\text{eff}}(\mu) \right\}, \quad (43)$$

$$P_8^q(K_0^*(1430)) = \frac{\alpha_e}{9\pi N_c} \left\{ (C_1(\mu) + N_c C_2(\mu)) \left[\frac{4}{3} \ln \frac{m_b}{\mu} + \frac{2}{3} - \hat{G}_{K_0^*(1430)}(s_q) \right] - 3C_{7\gamma}^{\text{eff}}(\mu) \right\}, \quad (44)$$

and

$$P_{10}^q(K_0^*(1430)) = \frac{\alpha_e}{9\pi N_c} \left\{ (C_1(\mu) + N_c C_2(\mu)) \left[\frac{4}{3} \ln \frac{m_b}{\mu} + \frac{2}{3} - \hat{G}_{K_0^*(1430)}(s_q) \right] - 3C_{7\gamma}^{\text{eff}}(\mu) \int_0^1 \frac{dx}{1-x} \Phi_{K_0^*(1430)}(x) \right\}. \quad (45)$$

Comparing Eq. (26) with Eqs. (30) and (41) with Eq. (45), one can see that the formal structures of $P_4^q(K_0^*(1430))$ and $P_{10}^q(K_0^*(1430))$ in terms of $C_n(\mu)$, of gluon kernel functions, $G_{M_2}(s_q)$ and of LCDA, $\Phi_{M_2}(x)$, where M_2 is now $K_0^*(1430)$ instead of $K^*(892)$, are identical to those of $P_4^q(K^*(892))$ and $P_{10}^q(K^*(892))$, respectively. The gluon kernel functions, entering in Eqs. (41)–(45), are

$$G_{K_0^*(1430)}(s_q) = \begin{cases} \frac{5}{3} + \frac{2i\pi}{3} + \frac{B_1^{K_0^*}(\mu)}{2}, & s_q = 0, \\ \frac{85}{3} - 6\sqrt{3}\pi + \frac{4\pi^2}{9} - \left[\frac{155}{2} - 36\sqrt{3}\pi + 12\pi^2 \right] B_1^{K_0^*}(\mu), & s_q = 1, \\ \frac{5}{3} - \frac{2}{3} \ln s_c + \frac{B_1^{K_0^*}(\mu)}{2} + \frac{4}{3} [8 + 9B_1^{K_0^*}(\mu)] s_c + 2[8 + 63B_1^{K_0^*}(\mu)] s_c^2 \\ - 306B_1^{K_0^*}(\mu) s_c^3 - \frac{2}{3} \sqrt{1-4s_c} [1 + 2s_c + 6(4 + 27B_1^{K_0^*}(\mu)) s_c^2 - 324B_1^{K_0^*}(\mu) s_c^3] \\ \times [2 \operatorname{arctanh}(\sqrt{1-4s_c}) - i\pi] + 12s_c^2 \left[1 + 3B_1^{K_0^*}(\mu) - \frac{4}{3}(1 + 9B_1^{K_0^*}(\mu)) s_c \right. \\ \left. + 18B_1^{K_0^*}(\mu) s_c^2 \right] [2 \operatorname{arctanh}(\sqrt{1-4s_c}) - i\pi]^2, & s_q = s_c, \end{cases} \quad (46)$$

and

$$\hat{G}_{K_0^*(1430)}(s_q) = \begin{cases} \frac{16}{9} + \frac{2\pi}{3} i, & s_q = 0, \\ \frac{-32}{9} + \frac{2\pi}{\sqrt{3}}, & s_q = 1, \\ \frac{16}{9} (1 - 3s_c) - \frac{2}{3} [\ln s_c + (1 - 4s_c)^{3/2} [2 \operatorname{arctanh}(\sqrt{1-4s_c}) - i\pi]], & s_q = s_c. \end{cases} \quad (47)$$

B. Vertex contributions

The relevant vertex corrections, $V_n(K_0^*(1430))$, for $n \in \{1, 4, 6, 8, 10\}$ are the following:

$$V_n(K_0^*(1430)) = \begin{cases} 12 \ln(\frac{m_b}{\mu}) - 3i\pi - \frac{37}{2} + \frac{1}{2}(11 - 6i\pi)B_1^{K_0^*}(\mu), & n \in \{1, 4, 10\}, \\ -6, & n \in \{6, 8\}, \end{cases} \quad (48)$$

with $\mu = m_b$.

C. Hard-scattering contributions

From gluon exchange between the scalar $K_0^*(1430)$ and the spectator u quark one derives, at $\mu = m_b/2$, the hard-scattering corrections. One writes it as in Eq. (34) with $M_2 \equiv K_0^*(1430)$ and $A_{\pi K_0^*(1430)}$ and $B_{\pi K_0^*(1430)}$ defined by Eqs. (14) and (21), respectively. Here

$$\tilde{H}_n(\pi K_0^*(1430)) = \begin{cases} \frac{3m_B}{\lambda_B} [3(B_1^{K_0^*}(\mu) + 1) - r_\chi^\pi(\mu)X_H(B_1^{K_0^*}(\mu) - 1)], & n \in \{1, 4, 10\}, \\ 0, & n \in \{6, 8\}. \end{cases} \quad (49)$$

As for the $K^*(892)$ (Sec. III C) the end-point divergence is modeled by X_H .

D. Annihilation contributions

The weak initial and final annihilation amplitudes, $A_j^I(\pi K_0^*(1430))$ and $A_j^F(\pi K_0^*(1430))$ (with $j = 1$ and 3) at $\mu = m_b/2$ are calculated starting from Ref. [2] for $B \rightarrow \pi K_0^*(1430)$:

$$\begin{aligned} A_1^I(\pi K_0^*(1430)) &\approx 2\pi\alpha_s(\mu)(9B_1^{K_0^*}(\mu)(3X_A + 4 - \pi^2) - r_\chi^\pi(\mu)r_\chi^{K_0^*}(\mu)X_A^2), \\ A_3^I(\pi K_0^*(1430)) &\approx 6\pi\alpha_s(\mu)\left\{3r_\chi^\pi(\mu)B_1^{K_0^*}(\mu)\left(X_A^2 - 4X_A + 4 + \frac{\pi^2}{3}\right) + r_\chi^{K_0^*}(\mu)\left(X_A^2 - 2X_A + \frac{\pi^2}{3}\right)\right\}, \\ A_3^F(\pi K_0^*(1430)) &\approx 6\pi\alpha_s(\mu)X_A\{r_\chi^\pi(\mu)B_1^{K_0^*}(\mu)(6X_A - 11) - r_\chi^{K_0^*}(\mu)(2X_A - 1)\}, \end{aligned} \quad (50)$$

with X_A an end-point divergence [Eq. (56)]. These amplitudes will then be implemented in the $b_n(\pi K_0^*(1430))$ given in Eqs. (22) and (23).

V. INPUT

A. Numerical parameters

In this section, one summarizes all the values of the parameters required for performing numerical applications. From Ref. [5], the meson masses in GeV are

$$\begin{aligned} m_B &= 5.300, & m_\pi &= 0.139, & m_K &= 0.493, \\ m_{K^*} &= 0.892, & m_{K_0^*} &= 1.430, & m_{B^*} &= 5.320. \end{aligned} \quad (51)$$

The running quark masses (at $m_b = 4.2$ GeV) in GeV are

$$\begin{aligned} m_b &= 4.2, & m_c &= 1.3, \\ m_s &= 0.070, & m_{u,d} &= 0.003, \end{aligned} \quad (52)$$

whereas at $m_b/2$, one has in GeV [7],

$$\begin{aligned} m_b &= 4.95, & m_c &= 1.51, \\ m_s &= 0.090, & m_{u,d} &= 0.005. \end{aligned} \quad (53)$$

The meson decay constants in MeV are

$$\begin{aligned} f_B &= 180 \pm 40 [6], & f_{K^*} &= 218 \pm 4 [2], \\ f_\pi &= 130 \pm 0.2 [5], & f_{K^*}^\perp &= 175 \pm 25 [2]. \end{aligned} \quad (54)$$

The scalar meson decay constant $f_{K_0^*}$, which appears in Eqs. (8), (14), and (21), does not, in fact, enter in our calculation as it cancels out in $\mathcal{A}_3(B \rightarrow \pi\pi K)$ [Eq. (4)], in $\beta_n(\pi M_2)$ [Eq. (20)], and in $H_n(\pi M_2)$ [Eq. (34)].

The B^\pm and B^0 mean lives, entering in Eq. (16), are [5] $\tau_{B^\pm} = (1.638 \pm 0.011) \times 10^{-12}$ s and $\tau_{B^0} = (1.530 \pm 0.009) \times 10^{-12}$ s, respectively.

For the Wilson coefficients, $C_n(\mu)$, we take, at both scales $\mu = m_b$ and $m_b/2$, the next-to-leading order logarithmic approximation values as given in Table 1 of Ref. [6]. Using Eqs. (18) and (19), one obtains, at the scale $\mu = m_b$, the universal LO $a_n^q(\mu)$ values presented in the first column of Table I.

TABLE I. Real and imaginary parts of the leading order (LO), vertex, penguin, and hard-scattering contributions to the short distance amplitude, $a_n^q(\mu)$, for P and S waves. The scale $\mu = m_b$ except for the hard scattering where $\mu = m_b/2$.

	LO	Vertex	P wave		Total
			Penguin	Hard scattering	
$a_1^u(\mu)$	(1.018; 0)	(0.028; 0.014)	(0; 0)	(-0.246; 0.317)	(0.800; 0.331)
$a_1^c(\mu)$					
$a_4^u(\mu)$	-0.031; 0)	(-0.002; -0.001)	(0.003; -0.014)	(0.018; -0.023)	(-0.012; -0.038)
$a_4^c(\mu)$			(-0.002; -0.005)		(-0.017; -0.029)
$a_6^u(\mu)$	(0; 0)	(0.0006; -0.001)	(-0.007; -0.0009)	(0; 0)	(-0.006; -0.002)
$a_6^c(\mu)$			(0.001; 0.011)		(0.002; 0.010)
$a_8^u(\mu)$	(0; 0)	$(-0.6; 1.3) \times 10^{-5}$	$(-4.7; 0) \times 10^{-5}$	(0; 0)	$(-5.3; 1.3) \times 10^{-5}$
$a_8^c(\mu)$			$(-0.3; 6.4) \times 10^{-5}$		$(-0.9; 7.7) \times 10^{-5}$
$a_{10}^u(\mu)$	(-0.0014; 0)	(0.0014; 0.0007)	(0.0002; -0.0001)	(-0.013; 0.016)	(-0.012; 0.017)
$a_{10}^c(\mu)$			(0.0002; -0.0001)		
S wave					
$a_1^u(\mu)$	(1.018; 0)	(-0.016; 0.089)	(0; 0)	(-0.151; 0.184)	(0.851; 0.273)
$a_1^c(\mu)$					
$a_4^u(\mu)$	(-0.031; 0)	(0.001; -0.007)	(0.023; -0.017)	(0.011; -0.014)	(0.004; -0.037)
$a_4^c(\mu)$			(0.039; 0.036)		(0.021; 0.016)
$a_6^u(\mu)$	(-0.039; 0)	(-0.0004; 0)	(-0.003; -0.014)	(0; 0)	(-0.042; -0.014)
$a_6^c(\mu)$			(-0.006; -0.004)		(-0.045; -0.004)
$a_8^u(\mu)$	$(44; 0) \times 10^{-5}$	$(0.4; 0) \times 10^{-5}$	$(4; -10) \times 10^{-5}$	(0; 0)	$(48; -10) \times 10^{-5}$
$a_8^c(\mu)$			$(2; -5) \times 10^{-5}$		$(46; -5) \times 10^{-5}$
$a_{10}^u(\mu)$	(-0.0014; 0)	(-0.0008; 0.005)	(0.0015; -0.0001)	(-0.008; 0.009)	(-0.009; 0.014)
$a_{10}^c(\mu)$			(0.0016; 0.0002)		(-0.009; 0.014)

B. Model parameters

For the $B \rightarrow \pi$ transition form factor, we employ the pole-extrapolation model [8],

$$F_0^{B \rightarrow \pi}(q^2) = \frac{f_0(0)}{(1 - \sigma_1 \frac{q^2}{m_{B^*}^2} + \sigma_2 \frac{q^4}{m_{B^*}^4})}, \quad (55)$$

at the momentum transfer, q . In the transition form factor model we are using, the numerical parameters are $f_0(0) = 0.29$, $\sigma_1 = 0.76$, and $\sigma_2 = 0.28$.

As pointed out in Sec. II, we use the vector $f_1^{\pi K}(q^2)$ and scalar $f_0^{\pi K}(q^2)$ (with $f_K/f_\pi = 0.193$) form factors derived in [3].

The hard-scattering and annihilation contributions for the $K^*(892)$ given in Eqs. (35) and (36) as well as those for the $K_0^*(1430)$ given in Eqs. (49) and (50) involve divergences, X_H and X_A , which are modeled [2] as follows:

$$X_{A,H} = (1 + \rho_{A,H} \exp(i\phi_{A,H})) \ln \frac{m_B}{\lambda_h}, \quad (56)$$

with, for each $X_{A,H}$, two real parameters $\rho_{A,H} > 0$ and $0 < \phi_{A,H} < 360^\circ$. One expects the annihilation and hard-scattering contributions to be of the order of $\ln(m_B/\lambda_h)$ with $\lambda_h = 0.5$ GeV (see Ref. [6]).

VI. RESULTS AND DISCUSSION

Within the QCDF approach including final state interactions, before and after hadronization, we fit, with the two complex parameters (ρ_A, ϕ_A) and (ρ_H, ϕ_H) the mass and helicity angle distributions, the P -wave branching ratios and the CP asymmetries provided by the Belle [9–12] and BABAR [13–16] Collaborations. We consider 206 effective mass distribution data, 82 helicity distribution points, 6 values of asymmetries for both $\pi K^*(892)$ and $\pi K_0^*(1430)$, and 4 branching ratios for $\pi K^*(892)$. Altogether we have 298 observables with equal weight. Note that in the fit we did suppress some points which lie outside the general trend of the data. We have checked that these suppressions do not influence the results of the fit.

We obtain a $\chi^2/\text{dof} = 492.5/(298 - 4) = 1.68$ with the values $\rho_H = 54.43 \pm 7.32$, $\phi_H = -0.95 \pm 0.10$ rad for the hard-scattering parameters and $\rho_A = 2.51 \pm 0.11$, $\phi_A = -2.98 \pm 0.06$ rad for the annihilation parameters. The corresponding hard-scattering, $H_n(M_2)$, contributions to the short distance amplitudes, $a_n^q(\mu)$ of Eq. (18), are listed in Table I together with the leading order, vertex $V_n(M_2)$ and penguin $P_n^q(M_2)$ contributions for the P and S waves. The resulting annihilation amplitudes, $\beta_n(\pi M_2)$, are displayed in Table II.

The amplitude, $a_n^q(\mu)$, for $n = 4$ –10 are always corrections to the $a_1^q(\mu)$. For $n = 1$ –8, the modulus of the LO contribution is larger than the modulus of the vertex term,

TABLE II. Real and imaginary parts of the annihilation contributions for P and S waves. Here $\mu = m_b/2$.

	P wave	S wave
$\beta_2(\pi M_2)$	(0.006; 0.0007)	(0.031; 0.013)
$\beta_3(\pi M_2)$	(-0.024; -0.011)	(0.094; 0.051)
$\beta_{3,EW}(\pi M_2)$	$(0.025; 0.005) \times 10^{-2}$	$(-0.009; -0.003) \times 10^{-2}$

itself larger than that of the penguin. The modulus of the hard-scattering contribution is in between 25% to 60% of the modulus of the LO term. The vertex, penguin, and hard-scattering contributions can be seen as corrections to the leading order amplitude whereas for $n = 10$, $H_n(M_2)$ gives the main contribution to the very small amplitude $a_{10}^q(\mu)$. The moduli of the annihilation terms (see Table II) are of the order of those of the vertex or penguin for both P and S waves.

Since the present work and that of Ref. [3] (see their Table VI) use the same leading and next-to-leading order parameters, the P -wave vertex and penguin contributions to the a_n^q are quite similar. For the S wave, there are some differences in these corrections for a_1^q and a_4^q . These arise from the introduction of Gegenbauer moments up to order 3 in Ref. [3]. The moduli of the a_1^q are about 20% smaller than those of Ref. [3] (see their Table I). This reduction comes mainly from the hard-scattering contributions.

The $K^\pm \pi^\mp$ effective mass distributions for $B^0 \rightarrow \pi^- \pi^+ K^0$ are globally well fitted: for \bar{B}^0 decay, $\chi_{\text{Belle}}^2/\text{dof} = 1.03$, $\chi_{\text{BABAR}}^2/\text{dof} = 0.71$ and for B^0 decay, $\chi_{\text{Belle}}^2/\text{dof} = 1.0$, $\chi_{\text{BABAR}}^2/\text{dof} = 2.96$. In the case of the

$B^\pm \rightarrow \pi^\pm \pi^\mp K^\pm$ effective mass distributions, one has $\chi_{\text{Belle}}^2/\text{dof} = 2.55$, $\chi_{\text{BABAR}}^2/\text{dof} = 2.65$, the data being not very well reproduced, in particular, for the charged B decays, below 0.9 GeV. The helicity angle distributions are well fitted for both decays with a χ^2/dof of the order of 1.

All the results on branching ratios and asymmetries are summarized in Table III. For the $K^*(892)$ branching ratios, 90% of the χ^2/dof comes from the B^0 and \bar{B}^0 BABAR data. These are incompatible with the corresponding ones from Belle. The P -wave experimental branching ratios for $B^\pm \rightarrow \pi^\pm \pi^\mp K^\pm$ are well reproduced whereas our predictions for the S -wave branching ratios do not fully agree with those provided by Belle but do agree better with the BABAR data. As discussed in detail in Ref. [3], the determination of the $B \rightarrow \pi K_0^*(1430)$ branching ratios is problematic as the $K_0^*(1430)$ resonance is wide and the result is quite model dependent. However, within the factorization and quasi-two-body hypotheses, the use of a scalar form factor, determined with precision from theory and experiments other than those of B decays, makes our $\pi K_0^*(1430)$ branching ratio predictions well founded.

It is difficult to draw any firm conclusions from the small asymmetries obtained from our global fit for both P and S waves since the experimental data have large uncertainties. We found that, if we introduced some factor in the χ^2 to increase the weight of the CP asymmetries, as done in Ref. [3], we obtain a fit of equivalent quality with, indeed, \mathbb{A}_{CP} values closer to the central values of the experimental analyses, in particular, for neutral B decays.

TABLE III. Branching fractions \mathcal{B} [see Eq. (16)] in units of 10^{-6} and direct CP asymmetries \mathbb{A}_{CP} in % [Eq. (17)] averaged over charge conjugate reactions. The values of the model, calculated by the integration of the $m_{\pi K}$ distribution over the $m_{\pi K}$ range from $m_{\pi K}^{\min} = 0.82$ to $m_{\pi K}^{\max} = 0.97$ GeV for the P wave and from 1.0 to 1.76 for the S wave are compared to the corresponding Belle and BABAR results given in the fourth column for \mathcal{B} and fifth column for \mathbb{A}_{CP} . Model uncertainties arise from the phenomenological parameter errors obtained through the minimization. The third column gives the model values without the phenomenological hard-scattering and annihilation contributions.

\mathcal{B} (decay channel)	Model	$H_n[\beta_n] \equiv 0$	$\mathcal{B}^{\text{exp}}(m_{\pi K}^{\min}, m_{\pi K}^{\max})$	\mathcal{B}^{exp}	Refs.
$\mathcal{B}(B^- \rightarrow \pi^- \bar{K}^{*0} \rightarrow \pi^- \pi K)$	5.82 ± 0.15	2.17	5.35 ± 0.59 5.98 ± 0.75	6.45 ± 0.71 7.20 ± 0.90	[10] [13]
$\mathcal{B}(\bar{B}^0 \rightarrow \pi^+ \bar{K}^{*-} \rightarrow \pi^+ \pi K)$	4.50 ± 0.21	1.65	4.65 ± 0.77 6.47 ± 0.72	5.60 ± 0.93 11.70 ± 1.30	[9] [16]
$\mathcal{B}(B^- \rightarrow \pi^- \bar{K}_0^{*0} \rightarrow \pi^- \pi K)$	12.11 ± 0.32	7.80	25.92 ± 2.45 17.64 ± 3.60	32 ± 3.02 24.5 ± 5.0	[10] [13]
$\mathcal{B}(\bar{B}^0 \rightarrow \pi^+ \bar{K}_0^{*-} \rightarrow \pi^+ \pi K)$	11.05 ± 0.25	7.45	24.95 ± 3.25 12.19 ± 3.26	30.80 ± 4.01 25.40 ± 6.80	[9] [14]
\mathbb{A}_{CP} (decay channel)	Model	$H_n[\beta_n](\pi M_2) \equiv 0$		$\mathbb{A}_{CP}^{\text{exp}}$	Refs.
$\mathbb{A}_{CP}(B^- \rightarrow \pi^- \bar{K}^{*0} \rightarrow \pi^- \pi K)$	0.89 ± 0.23	1.29		-14.90 ± 6.75 3.2 ± 5.4	[10] [13]
$\mathbb{A}_{CP}(\bar{B}^0 \rightarrow \pi^+ \bar{K}^{*-} \rightarrow \pi^+ \pi K)$	-0.99 ± 3.42	7.99		-14 ± 12 7.60 ± 4.66	[14] [10]
$\mathbb{A}_{CP}(B^- \rightarrow \pi^- \bar{K}_0^{*0} \rightarrow \pi^- \pi K)$	0.27 ± 0.10	0.27		3.20 ± 4.60 17.0 ± 26	[13] [14]
$\mathbb{A}_{CP}(\bar{B}^0 \rightarrow \pi^+ \bar{K}_0^{*-} \rightarrow \pi^+ \pi K)$	0.75 ± 0.90	-0.68			

The plots on effective mass and helicity angle distributions, almost identical to those published in [3], will not be given here. For the S wave and for $m_{\pi K} \lesssim 0.8$ GeV, the effective mass distributions, mainly for the charged B decays, are smaller than those of Ref. [3] which could indicate some stronger suppression of the $K_0^*(800)$ contribution.

In relation to the direct CP violation asymmetries, we will focus on the differential difference of effective mass branching ratio distributions for charge conjugate channels. In Fig. 1 we draw $d(\Delta\mathcal{B})/dm_{\pi K}$ with $\Delta\mathcal{B} = \mathcal{B}(B \rightarrow \pi\pi K) - \mathcal{B}(\bar{B} \rightarrow \bar{\pi}\bar{\pi}\bar{K})$ [numerator of \mathbb{A}_{CP} , see Eq. (17)] for the charged and neutral decays and calculated from the S , P , and $S + P$ amplitudes, where the strong interaction scalar and vector form factors have been factorized out. Figure 2 illustrates these distribution differences for the full $S + P$ amplitude including these form factors. The weak interaction plus the strong interaction before hadronization produces $S + P$ distribution differences (see Fig. 1) negative for $m_{\pi K}$ below ~ 1 GeV, positive and increasing above. Including the final state interaction after hadronization, the $S + P$ distributions as seen in Fig. 2 are enhanced in the vicinity of the $K^*(892)$ resonance, that of the charged channel is positive while that of the neutral is negative. The positive enhancement at the 1430 resonance for the B^0 decays is larger than that of the B^- .

The denominator of \mathbb{A}_{CP} giving a similar contribution for charged and neutral channels, the above behavior of the $S + P$ distributions allows us to understand the model values (calculated by integrating distributions over the $m_{\pi K}$ range quoted in the Table III caption) for \mathbb{A}_{CP} dis-

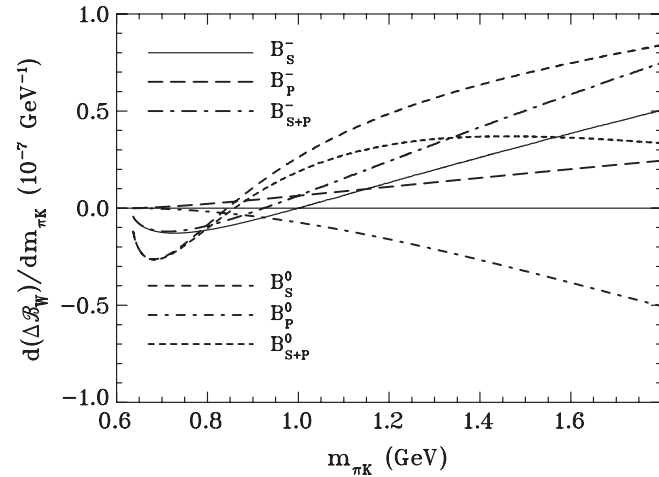


FIG. 1. Here $\Delta\mathcal{B}_W$ represent the contributions, to the numerator of the CP asymmetry parameter \mathbb{A}_{CP} of Eq. (17), of the different S , P , and $S + P$ amplitudes where the scalar and vector form factors have been factorized out. The curves denoted by $B_{S,P,S+P}^-$ correspond to the contribution for the S , P , and $S + P$ of this weak interaction plus perturbative QCD interaction amplitudes to the charged B decays and those denoted by $B_{S,P,S+P}^0$ the contributions to the neutral B decays.

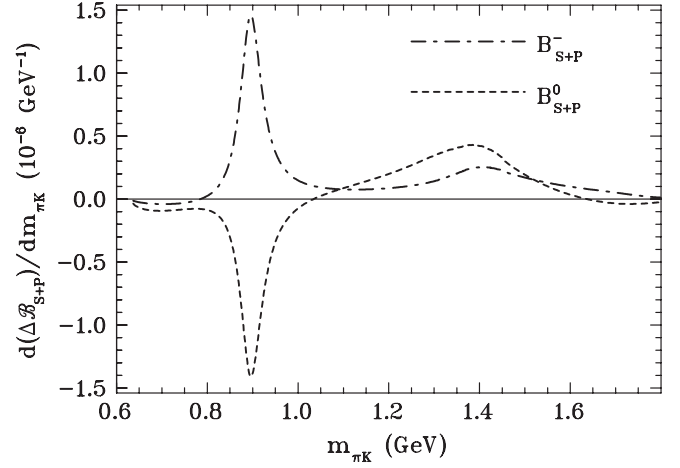


FIG. 2. As in Fig. 1 but only for the $S + P$ amplitudes including the scalar and vector form factor contributions.

played in Table III, knowing that the P -wave contribution dominates in the vector resonance region and the S wave in the scalar one. One can see that a strong final state interaction after hadronization can increase the CP asymmetry.

VII. SUMMARY AND OUTLOOK

In the present study, we analyze the K^* resonance effects on the direct CP violation in the $B \rightarrow \pi\pi K$ decay channels. We calculate the amplitudes for the $B^0 \rightarrow \pi^- \pi^+ K^0$ and $B^\pm \rightarrow \pi^\pm \pi^\mp K^\pm$ decays in the QCD factorization framework [2,6] at leading order in Λ_{QCD}/m_b and at the next-to-leading order in α_s . In order to do so, we approximate these three-body processes as quasi-two-body B decays into $\pi K^*(892)$ and $\pi K_0^*(1430)$ since these final state K^* resonances dominate the πK effective mass region below 2 GeV. All the contributions, before hadronization, i.e., from vertex, penguin, hard-scattering, and annihilation corrections as well as those after hadronization, i.e., from the K^* meson resonance formation and decay described by the strong interaction scalar and vector form factors, are included. We complete the calculation performed in Ref. [3] by adding explicitly the hard-scattering and annihilation contributions which are however subject to large uncertainties arising from the presence of end-point divergences. These divergences are modeled with two complex parameters; they are the sole fitted parameters entering in the present calculation. Thus, as compared to Ref. [3], our model involves only 4 real phenomenological parameters instead of 8 while reproducing equally well the present data. These 4 parameters are then determined through a fit to the available data on mass and helicity angle distributions, branching ratios, and CP asymmetries originating from Belle and BABAR Collaboration measurements. The large experimental uncertainties in CP asymmetries do not yield strong constraints. Producing higher statistics experimental data seem to us mandatory in order to improve

constraints on models. Furthermore, it should sort out the present discrepancies between the Belle and BABAR analyses.

At this stage one cannot conclude that the data are or are not compatible with the standard model. Yet, the possibility of new physics effects, as, for instance, in the minimal supersymmetric standard model approach studied in Ref. [17], cannot be excluded. However, the theoretical basis of our model being restricted to next-to-leading order corrections, the phenomenological terms can simulate next-to-next-to leading order (NNLO) effects. It could also take into account charming penguin contributions. In principle, the NNLO corrections to hard scattering are amenable to convergent integrals which can be evaluated [18,19]. This contribution could reduce the phenomenological part of our model amplitudes. The long distance charming penguin amplitudes such as those arising from intermediate $D_s^{(*)}D^{(*)}$ states could be important since the branching fractions for the transition $B \rightarrow D_s^{(*)}D^{(*)}$ are quite large. However, their contributions cannot be calculated in a QCD perturbative framework. Both NNLO corrections and charming penguin amplitudes should be included before being able to give a firm statement as to whether or not it is necessary to introduce new physics to understand the data, but, this is outside the scope of the present study.

In conclusion, from this analysis, we point out the important following aspects.

- (i) It constitutes a robust state of the art QCD factorization calculation at next-to-leading order in the strong coupling constant. In this framework, the strong phase can be generated dynamically. However, the mechanism suffers from end-point singularities which are not well controlled. It is now apparent that the Cabibbo-Kobayashi-Maskawa matrix is the dominant source of CP violation in flavor changing processes in B decays. The corrections to this dominant source coming from beyond the standard model are not expected to be large. In fact, the main remaining uncertainty lies in the factorization approximation which provides an explicit picture in the heavy quark limit. It takes into account all the leading contributions as well as subleading corrections to the naive factorization. The soft collinear effective theory (SCET) has been proposed as a new procedure for factorization [18]. It allows one to formulate a collinear factorization theorem in terms of effec-

tive operators where new effective degrees of freedom are involved, in order to take into account the collinear, soft, and ultrasoft quarks and gluons. Following such steps should improve further our knowledge of B physics and, eventually, hint at contributions from physics beyond the standard model.

- (ii) It illustrates explicitly how the strong final state interaction after hadronization can enhance CP violation asymmetries. The variation of the differential difference of effective mass branching ratio distribution for charge conjugate channels as a function of the πK invariant mass over the whole range of the $K^*(892)$ and $K_0^*(1430)$ resonances shows that mixing resonance effects, as those seen in Fig. 2, can be observed within a window of 100–200 MeV. With the new Large Hadron Collider (LHC) providing energy and accuracy (small energy bin), we believe that by exploring such windows the LHCb Collaboration should be in a position to perform accurate measurements of CP violation in B to $\pi\pi K$ decays.
- (iii) It confirms the advantage of using, as a consequence of QCD factorization, a scalar form factor to describe the $\pi K_0^*(1430)$ final state. The $K_0^*(1430)$ resonance is very wide and its nonresonant part is difficult to evaluate. Thus, the determination of the $B \rightarrow \pi K_0^*(1430)$ branching fractions within, in particular, the isobar model, leads to large uncertainties. As advocated in Ref. [3], a parametrization with this scalar form factor, precisely constructed from unitary coupled channel equations using experimental kaon-pion T -matrix elements together with chiral symmetry and asymptotic QCD constraints, should be used in experimental Dalitz plot analysis.

ACKNOWLEDGMENTS

We thank the nonparticipating authors of Ref. [3] for their kind support during the course of this work. This research has been financed in part by an IN2P3-CNRS theory grant for the project *Contraintes sur les phases fortes dans les désintégrations hadroniques des mésons B* and by the IN2P3-Polish Laboratories Convention (Project No. 08-127).

[1] M. Kobayashi and T. Maskawa, *Prog. Theor. Phys.* **49**, 652 (1973); N. Cabibbo, *Phys. Rev. Lett.* **10**, 531 (1963).
 [2] M. Beneke and M. Neubert, *Nucl. Phys.* **B675**, 333 (2003).

[3] B. El-Bennich, A. Furman, R. Kamiński, L. Leśniak, B. Loiseau, and B. Moussallam, *Phys. Rev. D* **79**, 094005 (2009).

- [4] B. Moussallam, *Eur. Phys. J. C* **53**, 401 (2008).
- [5] C. Amsler *et al.* (Particle Data Group), *Phys. Lett. B* **667**, 1 (2008).
- [6] M. Beneke, G. Buchalla, M. Neubert, and C. T. Sachrajda, *Nucl. Phys.* **B606**, 245 (2001).
- [7] H. Y. Cheng, C. K. Chua, and K.-C. Yang, *Phys. Rev. D* **73**, 014017 (2006).
- [8] D. Melikhov, *Eur. Phys. J. direct C* **4**, 1 (2002).
- [9] A. Garmash *et al.* (Belle Collaboration), *Phys. Rev. D* **75**, 012006 (2007).
- [10] A. Garmash *et al.* (Belle Collaboration), *Phys. Rev. Lett.* **96**, 251803 (2006).
- [11] K. Abe *et al.* (Belle Collaboration), [arXiv:hep-ex/0509001](https://arxiv.org/abs/hep-ex/0509001).
- [12] K. Abe *et al.* (Belle Collaboration), [arXiv:hep-ex/0509047](https://arxiv.org/abs/hep-ex/0509047).
- [13] B. Aubert *et al.* (BABAR Collaboration), *Phys. Rev. D* **78**, 012004 (2008).
- [14] B. Aubert *et al.* (BABAR Collaboration), *Phys. Rev. D* **78**, 052005 (2008).
- [15] B. Aubert *et al.* (BABAR Collaboration), *Phys. Rev. D* **73**, 031101 (2006).
- [16] B. Aubert *et al.* (BABAR Collaboration), [arXiv:0708.2097](https://arxiv.org/abs/0708.2097).
- [17] M. Beneke, Xin-Qiang Li, and L. Vernazza, *Eur. Phys. J. C* **61**, 429 (2009).
- [18] M. Beneke, *Nucl. Phys. B, Proc. Suppl.* **170**, 57 (2007).
- [19] M. Beneke, T. Huber, and Xin-Qiang Li, *Nucl. Phys.* **B832**, 109 (2010).